

## Author's Accepted Manuscript

Investigation of bonded hydrogen defects in nanocrystalline diamond films grown with nitrogen/methane/hydrogen plasma at high power conditions

C.J. Tang, Haihong Hou, A.J.S. Fernandes, X.F. Jiang, J.L. Pinto, H. Ye

PII: S0022-0248(16)30909-5  
DOI: <http://dx.doi.org/10.1016/j.jcrysgro.2016.12.050>  
Reference: CRY23909

To appear in: *Journal of Crystal Growth*

Received date: 30 September 2016  
Revised date: 6 December 2016  
Accepted date: 14 December 2016

Cite this article as: C.J. Tang, Haihong Hou, A.J.S. Fernandes, X.F. Jiang, J.L. Pinto and H. Ye, Investigation of bonded hydrogen defects in nanocrystalline diamond films grown with nitrogen/methane/hydrogen plasma at high power conditions, *Journal of Crystal Growth*, <http://dx.doi.org/10.1016/j.jcrysgro.2016.12.050>

This is a PDF file of an unedited manuscript that has been accepted for publication. As a service to our customers we are providing this early version of the manuscript. The manuscript will undergo copyediting, typesetting, and a review of the resulting galley proof before it is published in its final citable form. Please note that during the production process errors may be discovered which could affect the content, and all legal disclaimers that apply to the journal pertain

# Investigation of bonded hydrogen defects in nanocrystalline diamond films grown with nitrogen/methane/hydrogen plasma at high power conditions

C.J. Tang<sup>a,b,\*</sup>, Haihong Hou<sup>a</sup>, A.J.S. Fernandes<sup>b</sup>, X.F. Jiang<sup>a</sup>, J.L. Pinto<sup>b</sup>, H. Ye<sup>c</sup>

<sup>a</sup>Department of Physics, Jiangsu Key Laboratory for Advanced Functional Materials, Changshu Institute of Technology, Changshu 215500, Peoples R China

<sup>b</sup>Department of Physics, I3N (Institute for Nanostructures, Nanomodelling and Nanofabrication), University of Aveiro, Campus Universitário de Santiago, 3810-193 Aveiro, Portugal

<sup>c</sup>School of Engineering and Applied Science, Aston University, Aston Triangle, Birmingham, B4 7ET, UK

\*Corresponding author. Tel: +351-234-370356; Fax: +351-234-378197. tang.chunjiu@ua.pt

## Abstract

In this work, we investigate the influence of some growth parameters such as high microwave power ranging from 3.0 to 4.0 kW and N<sub>2</sub> additive on the incorporation of bonded hydrogen defects in nanocrystalline diamond (NCD) films grown through a small amount of pure N<sub>2</sub> addition into conventional 4% CH<sub>4</sub>/H<sub>2</sub> plasma using a 5 kW microwave plasma CVD system. Incorporation form and content of hydrogen point defects in the NCD films produced with pure N<sub>2</sub> addition was analyzed by employing Fourier-transform infrared (FTIR) spectroscopy for the first time. A large amount of hydrogen related defects was detected in all the produced NCD films with N<sub>2</sub> additive ranging from 29 to 87 μm thick with grain size from 47 nm to 31 nm. Furthermore, a specific new H related sharp absorption peak appears in all the NCD films grown with pure N<sub>2</sub>/CH<sub>4</sub>/H<sub>2</sub> plasma at high powers and becomes stronger at powers higher than 3.0 kW and is even stronger than the 2920 cm<sup>-1</sup> peak, which is commonly found in CVD diamond films.

Based on these experimental findings, the role of high power and pure nitrogen addition on the growth of NCD films including hydrogen defect formation is analyzed and discussed.

**Keywords:** A1. Defects; A1. Nanostructures; A3. Microwave plasma chemical vapour deposition processes; B1. Diamond; B1. Nanomaterials

## 1. Introduction

Hydrogen in diamond has long been a research topic along the development of synthetic diamond either by chemical vapour deposition (CVD) or high-pressure high-temperature (HPHT) methods. Hydrogen and nitrogen are the most studied point defects in diamond [1-4], because they can drastically influence its electrical and electronic properties. For example, recent theoretical works have shown that hydrogen has surprising stability as a neutral interstitial impurity in diamond [1] and can co-exist with vacancy [2]. Furthermore, hydrogen even can form a complex defect together with nitrogen and vacancy [3].

Commonly a few percentage of  $\text{CH}_4$  (typically 1%-5%) diluted in  $\text{H}_2$  has been used as reactant gases for the growth of diamond by CVD methods [5]. Therefore, it is well recognized that hydrogen (in the gas phase) plays a significant role on the conventional growth of CVD diamonds. On the other hand, due to the rich hydrogen atmosphere within the CVD growth process, hydrogen is also simultaneously incorporated into the growing diamond product as a unavoidable impurity to some extent, which strongly depends on the overall growth conditions [6-16].

Recently the electrical and electronic properties of N-doped diamond thin films grown by using  $\text{CH}_4/\text{H}_2/\text{N}_2$  plasma CVD have been an important topic of research [17-20]. It is worth to mention that nitrogen must be included in the source reactant gases when N-containing diamond

such as N-doped NCD [15,21] or diamond possessing nitrogen-vacancy (NV) centres grown by CVD methods [22]. It has been demonstrated that N-doped NCD films fabricated by  $\text{CH}_4/\text{H}_2/\text{N}_2$  plasmas without Ar are favourable for achieving high-performance diamond-based optoelectronic devices [20]. Furthermore, very recently it has been reported that thin nanocrystalline CVD diamond films of 2.5  $\mu\text{m}$  thick deposited by using a small amount of  $\text{N}_2$  addition into  $\text{CH}_4/\text{H}_2$  plasma were applied in MEMS resonators and Young's Moduli of the obtained thin NCD films were between 840-920 GPa reaching 90% of that of the bulk diamond material [19]. Therefore, from the above-mentioned studies it can be concluded that NCD films grown with  $\text{CH}_4/\text{H}_2/\text{N}_2$  plasmas are suitable for device applications.

Considering the bottom-up growth nature of CVD diamond, it is easy to understand that morphology, microstructure and defect formation of N-doped NCD films, which are strongly dependent on the overall growth conditions, would thus have strong impact on the electrical and electronic properties of N-doped NCD films, and thus affect the final device performances too. In order to design and obtain optimum nanomaterials for high-performance diamond-based optoelectronic devices, it is desirable to have knowledge about the relation between the growth and properties of CVD diamonds. Therefore, it is necessary and important to study the relationship between the growth parameters and defect formation such as hydrogen and nitrogen in order to tailor the growth of N-doped NCD for device applications. However, so far there has yet study about hydrogen defects formed in N-doped NCD films, not even about the role of hydrogen defects on the electrical or electronic properties of N-doped NCD films.

It is well-known that in comparison with low power ( $\ll 3$  kW) microwave plasma CVD (MPCVD), high pressure high power MPCVD systems are efficient for producing high quality diamond films of high uniformity, large area and high growth rate [23-27]. Therefore, previously we have explored the advantages of high power plasma to achieve fast fabrication of N-doped NCD films using conventional 4%  $\text{CH}_4/\text{H}_2/$  plasma through only a small amount of  $\text{N}_2$  addition

[28]. In this work we investigate the impact of the growth parameters such as high microwave power and the amount of nitrogen addition on the formation of hydrogen defects for the first time in such N-doped NCD films grown with pure  $N_2/CH_4/H_2/$  plasma. The form and content of bonded hydrogen defects in the NCD films was investigated by using FTIR spectroscopy. The new experimental finding such as the appearance of the specific new hydrogen related infrared absorption peak at  $2834\text{ cm}^{-1}$  in all the NCD films grown with pure  $N_2$  addition at high powers shed light into the key role of high microwave power on the growth of CVD diamond films upon a small amount of nitrogen addition and the incorporation mechanism of hydrogen impurity in NCD films.

## 2. Experimental procedure

The new N-doped NCD samples investigated here were produced on (100) square silicon slices of  $25\times 25\times 1\text{ mm}^3$  using  $CH_4/H_2/N_2$  gases at powers from 3.0 to 4.0 kW in a 5 kW ASTeX PDS-18 MPCVD reactor and named as ND1 to ND3. The other operating parameters were kept constantly such as pressure 105 Torr and 4%  $CH_4$  in  $H_2$ . For each deposition, the Si substrate was directly placed on the centre of a Mo holder (5.08 cm in diameter and 3.55 mm thick), whose temperature was monitored by a thermocouple embedded into the water cooled holder stage. The thermocouple readings during diamond deposition were  $308\text{ }^\circ\text{C}$  for ND1,  $349\text{ }^\circ\text{C}$  for ND2, and  $372\text{ }^\circ\text{C}$  for ND3, respectively. The deposition time was 5.25 hour for sample ND1, 5.58 hour for ND2 and 4.67 hour for ND3. The detailed identification of the NCD nature of the samples by Raman spectroscopy and XRD has been reported [28]. For convenience of comparison and discussion, some growth parameters of the samples such as microwave power and the amount of  $N_2$  are listed in Table 1 together with some characteristics of the diamond films, such as average grain size, growth rate, and film thickness, which was measured by optical

microscopy using a micrometer ruler, with an error about  $\pm 10 \mu\text{m}$  due to non-homogeneity in film thickness coming from the growth process as well.

In order to check the reproducibility and comparison of the growth of NCD films through a small amount of  $\text{N}_2$  addition under similar conditions, a previous film was added here as ND4, which was grown at power 3.0 kW by using the same operating parameters as that for sample ND1, but on much bigger and thicker Si substrate, which can lead to a much higher substrate surface temperature than that of sample ND1 during growth. The Si substrate was a big silicon (100) wafer of 5.08 cm in diameter and 3.26 mm thick and put directly on the matched water cooled Mo holder, whose temperature measured by a thermocouple during the deposition was  $296^\circ\text{C}$ . The growth and characterization by using SEM, Raman and XRD of this sample has been reported [29].

The morphologies of the diamond films were characterized by using a Hitachi S-4100 scanning electron microscope (SEM) operated at 25 kV. The original middle infrared transmittance spectra with  $4 \text{ cm}^{-1}$  resolution of the NCD films (still on Si substrates) were obtained at normal incidence in an evacuated chamber of an IFS 66V FTIR spectrometer manufactured by Bruker Optics. A KBr beam-splitter and a DTGS detector with KBr window were used to cover the frequency range  $400 - 4000 \text{ cm}^{-1}$ .

### 3. Results and discussion

Top morphological characterization of the new N-doped NCD films ND1 to ND3 grown at power from 3.0 to 4.0 kW with slightly different amounts of  $\text{N}_2$  additive is shown in Fig. 1. From the high resolution SEM micrographs, a common feature can be clearly summarized for all the samples, namely they are composed by large clusters that consist of fine grains, whose sizes are within 100 nm, evidencing the nanocrystalline nature of the diamond films. Of course, some

morphological differences mainly on the shape of the granular structure and microstructure among the samples are also distinguishable when the power increases from 3.0 to 4.0 kW. For film ND1 grown at 3.0 kW with 1.0 sccm N<sub>2</sub>, the large clusters shown in Fig. 1 a and b look like big pyramids piled by many small brick-like units with {100} square like facet on the top; while a typical cauliflower like morphology composed by large clusters, that are commonly observed for most NCD films reported in the literature, is demonstrated in Fig. 1 c and d for film ND2 grown at 3.5 kW with 1.6 sccm N<sub>2</sub>. For film ND3 grown at 4.0 kW with 1.6 sccm N<sub>2</sub>, a relative smooth top morphology and smaller clusters in comparison with that of films ND1 and ND2 can be observed in Fig. 1 e and f, and the much higher magnification SEM micrograph (Fig. 1f) clearly demonstrates many {111} faceted small pyramids or crystallites of size ranging from several tens of nm up to 100 nm with sharp edges and rough surface. The different growth characteristics of the N-doped NCD films, of course are due to the various growth conditions employed.

The FTIR absorption spectra of the as-grown NCD films are given in Fig. 2. From Fig. 2, three major features can be clearly seen in the spectra. First, in the low-frequency region a strong interference pattern below 1800 cm<sup>-1</sup> can be immediately seen in the spectra of all the samples. This is due to the transparency of the thin NCD films. Generally using this interference pattern the film thickness can be calculated. However taking into account of the influence of surface roughness, grain size and non-diamond component on the transmittance measurement, for films thicker than 30 microns, this method is not suitable for thickness measurement.

Second, a strong absorption band between 1000 and 1400 cm<sup>-1</sup> with maximum roughly around 1250 cm<sup>-1</sup> still can be obviously distinguished in all the N-doped NCD samples despite of the strong interference patterns in the low frequency region. It is noteworthy to mention that for pure diamond single crystal, no first order absorption processes is active due to high symmetry of diamond [30]. The strong absorption band in the one-phonon region of the N-doped NCD

films is due to the presence of impurities, lattice defects, grain boundaries, and strain in the films, which can break the symmetry of the lattice and activate one-phonon absorption processes.

In comparison with single crystal, NCD films have intrinsic defect namely a large amount of grain boundaries due to small grain size in the nanometer range. Obviously as illustrated by SEM micrographs shown in Fig. 1, a large amount of grain boundaries due to the fine grain structure indeed exist in the N-doped NCD films. In addition, Raman spectra of the N-doped NCD films [28] have also shown the broadening of the diamond Raman peak at  $1332\text{ cm}^{-1}$ , indicating the presence of diamond lattice defects, and a broad absorption band around  $1500\text{ cm}^{-1}$  due to the coexistence of non-diamond component in the films. Furthermore, it has also been shown that nano-diamond crystals contain a high density of lattice defects such as stacking fault, and twin boundaries besides the high density of grain boundaries by TEM inspection [31]. Even for heteroepitaxial diamond film, recent TEM observation has also shown the existence of a large amount of dislocation in such high quality CVD diamond [32]. As for what kind absorption peaks in the one-phonon region corresponding to what kind defects in the NCD samples, detailed study of the one-phonon absorption is under way.

Third, in Fig. 2, a huge absorption band can be obviously seen between  $2700$  and  $3100\text{ cm}^{-1}$ , in the three-phonon region, namely the well-known CH stretching band, which is due to hydrogen related defects formed in the N-doped NCD films. Here, we first focus on the comparison of the shape and size of the CH stretching band of the N-doped NCD films. From Fig. 2, one can see that in general, the shape and size of the CH stretching band varies from samples. This means that the incorporation form and content of H defects strongly depends on the overall growth conditions. The huge CH stretching band also evidences that a large amount of H impurity was incorporated into the N-doped NCD films, in comparison with high quality large-grained polycrystalline CVD diamond films, which only have a little amount of H defects [16,33].



The different shape of the CH stretching band is caused by the changes in the intensity of sharp peaks within the band. This also indicates that the incorporation form and content of H defects changes too. In order to better compare the fine structure and relative intensity of different absorption peaks within the CH stretching band of the N-doped NCD films, the CH band is enlarged and shown in Fig. 3. The sharp peaks that can be clearly observed within the CH stretching band of samples ND1 to ND3 are summarized in Table 2 for clarity and comparison. It is worth to mention that besides the sharp peaks attributed to  $sp^3CH_x$  ( $x=1,2,3$ ), namely 2848 and 2920 are the symmetric and asymmetric C-H stretching mode of  $sp^3CH_2$ , while 2860 is the symmetric stretching mode of C-H in  $sp^3CH_3$ , and 2880 is the stretching mode of C-H in  $sp^3CH$  [14], the origin of the new sharp peak at about  $2833\text{ cm}^{-1}$  has not yet clearly identified. From Fig. 3 and Table 2, one can see that three sharp peaks at around 2833, 2880, and  $2920\text{ cm}^{-1}$  are commonly observed in all the new N-doped NCD films. The  $2920\text{ cm}^{-1}$  peak is most commonly observed in CVD diamonds [7-9,16] of various quality ranging from high quality transparent to poor quality back [33], and fine-grained NCD films [16,34] and appears strong in most cases, no matter the size of the CH stretching band. In addition, it also appears strong in single diamond crystal co-doped with H synthesized by HPHT method [35]. Therefore, in order to analyze the effect of growth parameters on the  $2833\text{ cm}^{-1}$  peak, we compare it with the common  $2920\text{ cm}^{-1}$  peak. Furthermore, by this way, the disturbance of other factors on the  $2833\text{ cm}^{-1}$  peak can be minimized because they were measured exactly under the same conditions. The intensity ratio of  $2833$  to  $2920\text{ cm}^{-1}$  peak is given in Table 1 too for further analysis. From Table 1, one can see clearly that the  $2833\text{ cm}^{-1}$  peak is even higher than the  $2920\text{ cm}^{-1}$  peak in all the N-doped NCD films grown at high powers.

It is worth to mention that free H in the NCD films either at surface or in the grain boundaries is not detected by FTIR. So far it is not possible to know or detect any quantitative correlation between the integrated area of the CH stretching band and the total amount of bonded

H in CVD diamond films, not even a clear understanding about the amount of each specific form of H within the CH stretching band such as  $sp^3CH_2$  (sym.  $2850\text{ cm}^{-1}$ , asym.  $2920\text{ cm}^{-1}$ ),  $sp^3CH_3$  (sym.  $2870\text{ cm}^{-1}$ , asym.  $2960\text{ cm}^{-1}$ ) and  $sp^3CH$  ( $2880\text{ cm}^{-1}$ ) [9-14]. Despite of such uncertainty, it has been shown that in general, the larger the integrated area of the CH stretching band, the higher amount of infrared active bonded H impurity in the CVD diamond films [8]. In order to roughly analyze the effect of high power and  $N_2$  addition on the total amount of infrared active bonded hydrogen in N-doped NCD films, we calculated the integrated area of the CH stretching band marked as  $A_{CH}$  (starting from  $2780\text{ cm}^{-1}$  and ended at  $3100\text{ cm}^{-1}$  and using a linear base line marked as dotted line in Fig. 3) and divided by the film thickness ( $t$ , unit cm) to reveal the characteristics of the material and listed them in Table 1 for comparison. From Table 1, one can see clearly that all the N-doped NCD films have  $A_{CH}/t$  higher than 10k, indicating a large amount of H impurity, while high quality transparent large-grained CVD diamond films have  $A_{CH}/t$  only about several tens [33]. We will further discuss qualitatively the specific influence of microwave power and the amount of  $N_2$  on H incorporation in N-doped NCD films later based on the present work and our previous work together.

In order to separate the ripple effect of thin films in the high frequency region on the clarification of the peaks within the CH stretching band, we show here the FTIR spectrum in Fig. 4a of the thick film ND4 of  $87\text{ }\mu\text{m}$  in thickness grown at 3.0 kW with 1.0 sccm  $N_2$  on much thicker Si substrate for comparison. From Fig. 4a, one can see clearly the strong absorption band in the one-phonon region below  $1500\text{ cm}^{-1}$  and the huge CH stretching band between  $2780$  and  $3100\text{ cm}^{-1}$  in the three-phonon region without having any noticeable ripple effect. In order to clearly identify the sharp peaks within the CH stretching band we enlarge the top part of the CH stretching band after removing the absorption background by choosing a linear baseline marked as dot line in Fig. 4a and shown in Fig. 4b. From Fig. 4b, one can see obviously that the sharp  $2833\text{ cm}^{-1}$  peak is the strongest among all the peaks within the band, of course including the

2920  $\text{cm}^{-1}$  peak. This result confirms the observation of this new peak in all the NCD films grown with  $\text{N}_2$  additive at high powers ( $\geq 3.0$  kW). The  $A_{\text{CH}}$  of film ND4 is also calculated using the linear baseline mentioned above and listed in Table 1 for comparison too.

In short, the present findings that N-doped NCD films contain a large amount of H impurity is consistent with our previous results that there are a large amount of H impurity in NCD films growth with simultaneous  $\text{N}_2$  and  $\text{O}_2$  or air addition using the same MPCVD reactor [34,36,37].

In the following, we analyze and discuss the impact of the main operating parameters such as high microwave power and  $\text{N}_2$  additive on the incorporation of hydrogen impurity in N-doped NCD films by combing the current experimental findings with our previous work and some literature work. Please keep in mind that just like diamond growth by CVD methods is the overall effect of all the growth parameters, H impurity incorporation in CVD diamond films is also the consequence of all the growth parameters.

First, it is well-known that substrate temperature is a key parameter for CVD diamond growth, however, in high power ( $\geq 3$  kW) MPCVD systems, it is not an independent operating parameter and is mainly tuned by microwave power (the increase of microwave power simultaneously leads to rise of substrate temperature because of direct plasma heating). In our present work, one can see that the Mo holder temperature rises from 308 °C through 349 °C to 372 °C with power increasing from 3.0 through 3.5 to 4.0 kW. The surface temperature ( $T_s$ ) of the 1 mm thick Si substrate is always much higher than that of the water cooled Mo holder. Although we could not directly measure the absolute Si substrate surface temperature during deposition, we can compare the relative difference between Si substrate surface temperatures that really matter for considering the role of microwave power on H incorporation, based on the temperature difference between the Mo holder during diamond deposition. Assuming that the thermal dispassion from the Si substrate to the Mo holder keeps constant under different growth conditions, the  $T_s$  difference between Si substrates is higher than (at least equal to) that of the

difference between the corresponding Mo substrate holders. Thus one can deduce that the  $T_s$  of the Si substrate at 4.0 kW should be at least 64 °C higher than that at 3.0 kW when microwave power increases from 3.0 to 4.0 kW, the temperature of the Mo holder raises 64 °C. This is consistent with other literature work. For example, it has been reported that for a 10 kW 2450 MHz MPCVD reactor, when microwave power increases from 2.5 to 4 kW, the substrate temperature, which also depends on the pressure used, can raise at least 100 °C [38]. The temperature difference of the Mo holder during diamond deposition at various powers is given in Table 3 for comparison.

In addition, when power is constant, we also can use Si substrates of different thickness to change the heat dissipation path and thus can adjust the Si substrate surface temperature which is the real temperature for diamond growth. This is the case of samples ND1 and ND4. For sample ND4, the temperature gradient and distribution along the 3.0 mm thickness direction has been analyzed by using finite element method previously [39]. Based on that temperature simulation results, we can estimate the surface temperature difference between ND4 and ND1 is about 116 °C, which is also listed in Table 3 for comparison.

Based on the present work, we can summarize the qualitative effect of high microwave power (MP) and its associated substrate temperature ( $T_s$ ) and the amount of  $N_2$  additive on the amount of H incorporated in NCD films in Table 3 by making four types of comparison of the experimental results listed in Table 1, namely (1) ND2 versus ND1, (2) ND3 versus ND1, (3) ND3 versus ND2, and (4) ND4 versus ND1.

In addition, in Table 3 we also added our previous relevant work as follows for comparison and deep understanding of the present experimental results.

(1) About the impact of microwave power on H incorporation in NCD films grown with  $N_2/O_2$  additives, when the amount of  $N_2$  and  $O_2$  addition (through 1.0 sccm air addition) was kept constant, with increasing microwave power ranging from 2.0 to 3.2 kW, H content

decreases while the new sharp peak at  $2834\text{ cm}^{-1}$  appears at much higher power (above 2.5 kW) [36]. It is worth to mention that the methane concentration (3.75% to 4%) and pressure (90 to 105 Torr) were adjusted slightly according to the corresponding level of microwave power, because in general higher power needs higher pressure to stabilize the plasma ball within the reaction chamber.

(2) About the effect of  $\text{N}_2$  additive on H defects in NCD films grown with  $\text{N}_2/\text{O}_2$  additives, when most operating parameters were kept constantly, such as microwave power 3.0 kW, pressure 105 Torr and 4%  $\text{CH}_4/\text{H}_2$  (the same as that for ND1, but the Si substrates were much thicker (the same as that for ND4), the total amount of  $\text{N}_2$  and  $\text{O}_2$  additive was also kept constantly at 1.0 sccm, with increasing the amount of  $\text{N}_2$  (from 0 to 1.0 sccm) (simultaneously  $\text{O}_2$  from 1.0 sccm down to 0), we have found that the total amount of bonded H impurity increases in the produced diamond films ranging from microcrystalline to nanocrystalline [37]. Please note that there the Si substrate surface temperature can be considered as constant, because both the microwave power and the thickness of the Si substrates were constant.

Based on Table 3, we can conclude definitively that increasing microwave power from 2.0 to 4.0 kW leads to H impurity in NCD films grown with  $\text{N}_2$  additive (either together with or without  $\text{O}_2$ ) decreases, while increasing the amount of  $\text{N}_2$  additive always results in increment of H defects in the growing NCD films.

Now let us we analyze the key effect of high microwave power on the specific incorporation form of H related defects in N-doped NCD films. For example, in the present work we found that the specific sharp peak at  $2833\text{ cm}^{-1}$  appears in all the N-doped NCD films grown at high powers ( $\geq 3\text{ kW}$ ). It was first found in the FTIR spectra of our NCD films grown with nitrogen and oxygen addition at 3.2 kW [34], while recently, we have also found that it does not appear in NCD samples grown at 2 kW on Si substrates with a small amount of nitrogen and oxygen or air addition (0.12% or higher) with methane concentration 4-5% using the same

MPCVD reactor [36]. Therefore, we can conclude that N<sub>2</sub> addition and high microwave power (> 2.0 kW) are the key growth parameters that responsible for the appearance of such peak. First, the present findings provide experimental evidence for further study of the origin and fine structure of such peak. Second, in turn, further understanding of high microwave power on the growth mechanism of NCD films upon a small amount of N<sub>2</sub> addition can be facilitated when the origin and fine structure of such peak can be clearly identified.

Then we briefly discuss the “invisible” impact of high microwave power on diamond growth and H incorporation through intermediate process such as gas phase chemistry and substrate surface chemistry based on some literature work through computer simulation of microwave plasma of CH<sub>4</sub>/H<sub>2</sub> and with N<sub>2</sub> [5,40-42]. In the present study, the amount of hydrogen and methane was kept constant at 4% CH<sub>4</sub>/H<sub>2</sub>, with increasing power from 3.0 to 4.0 kW, the density of both H atom and CH<sub>3</sub> radical should increase significantly due to much higher gas temperature (above 3200 K). Based on the above mentioned work, we can have the following possible deduction that in our high power (> 2 kW) conditions, the small amount of nitrogen added into the gas phase may also completely dissociate and new N related radicals such as N, CN, NH and NH<sub>2</sub> are created and may compete with CH<sub>x</sub> (x=0-3) growth species, and thus they may also have a certain possibility to be trapped in the growing diamond films as an impurity to some extent. In turn, the appearance of new infrared absorption peak at 2834 cm<sup>-1</sup> under high power conditions may be evidence of formation of H and N related defects in N-doped NCD films. In order to clarify the role of high microwave power on diamond growth by MPCVD, further study of H and N related defects formed in N-doped NCD films is under way.

#### 4. Conclusions

In summary, the influence of high microwave power ranging from 3.0 to 4.0 kW and a small amount of N<sub>2</sub> addition on the formation of hydrogen defects in NCD films grown with conventional 4% CH<sub>4</sub>/H<sub>2</sub> plasma in a 5 kW MPCVD reactor has been investigated. In generally, all NCD films grown with a small amount of nitrogen addition at high powers ( $\geq 2$  kW) have a large amount of bonded hydrogen defects. Higher microwave power has significantly influence on the incorporation form of bonded hydrogen defects in NCD films grown with N<sub>2</sub> addition. For example, at high powers ( $\geq 3.0$  kW), the new specific H related sharp absorption peak at 2834 cm<sup>-1</sup> appears in the NCD films grown with pure nitrogen addition and becomes stronger with increasing of power and is even stronger than the 2920 cm<sup>-1</sup> peak, which is commonly found in CVD diamond films. Further study is necessary in order to identify the origin and fine structure of this new absorption peak,

## Acknowledgement

This work was supported by the National Science Foundation (NSF) of China under grant No. 51102027. This work was also partially supported by project UID/CTM/50025/2013 funded by national funds through FCT - Portuguese Science and Technology Foundation. In addition, we also acknowledge the partial financial support by the European Union under Grant Agreement 295208 (CarbonNASA). The Project was also partially sponsored by the Scientific Research Foundation for the Returned Overseas Chinese Scholars, State Education Ministry. The authors thank Dr. Luís Vieira and Prof. Luís Robeiro of Department of Physics of University of Minho for their kind help on the FTIR measurements.

## References

[1] J.L. Lyons, C.G. Van de Walle, J. Phys. Cond. Matter. 28 (2016) 06LT01.

- [2] C.V. Peaker, J.P. Goss, P.R. Briddon, A.B. Horsfall, M.J. Rayson, *Phys. Status Solidi A* 212 (2015) 2431.
- [3] C.V. Peaker, J.P. Goss, P.R. Briddon, A.B. Horsfall, M.J. Rayson, *Phys. Status Solidi A* 212 (2015) 2616.
- [4] Sh. Michaelson, O. Ternyak, A. Hoffman, Y. Lifshitz, *Appl. Phys. Lett.* 90 (2007) 031914.
- [5] W.J. Rodgers, P.W. May, N.L. Allan, J.N. Harvey, *J. Chem. Phys.* 142 (2015) 214707.
- [6] C. Liu, X. Xiao, J. Wang, B. Shi, V.P. Adiga, R.W. Carpick, J.A. Carlisle, O. Auciello, J. *Appl. Phys.* 102 (2007) 074115.
- [7] K.M. McNamara, D.H. Levy, K.K. Gleason, C.J. Robinson, *Appl. Phys. Lett.* 60 (1992) 580-582.
- [8] K.M. McNamara, K.K. Gleason, C.J. Robinson, *J. Vac. Sci. Technol. A* 10 (1992) 3143-3148.
- [9] B. Dischler, C. Wild, W. Müller-Sebert, P. Koidl, *Physica B* 185 (1993) 217-221.
- [10] A. Kimura, Y. Nakatani, K. Yamada, T. Suzuki, *Diamond Relat. Mater.* 8 (1999) 37-41.
- [11] S.A. Rakha, Jianqing Cao, Huihao Xia, Guojun Yu, Dezhong Zhu, Jinlong Gong, *Diamond Relat. Mater.* 18 (2009) 1247.-1252.
- [12] Sh. Michaelson, O. Ternyak, A. Hoffman, Y. Lifshitz, *Appl. Phys. Lett.* 90 (2007) 031914.
- [13] X. Jiang, P. Willich, M. Paul, C-P. Klages, *J. Mater. Res.* 14 (1999).3211-3220.
- [14] KM. McNamara, B. E. Williams, K.K. Gleason, B.E. Scruggs, *J. Appl. Phys.* 76 (1994) 2466-2472.
- [15] M.S. Haque, H.A. Naseem, J.L. Shultz, W.D. Brown, *J. Appl. Phys.* 83 (1998) 4421-4429.
- [16] C.J. Tang, M.A. Neto, M.J. Soares, A J.S. Fernandes, A.J. Neves, J. Grácio, *Thin Solid Films* 515 (2007) 3539-3546.
- [17] M. Fick, K.J. Sankaran, J. Ryl, R. Bogdanowicz, I.N. Lin, K Haenen, K. Darowicki., *Appl. Phys. Lett.* 108, (2016) 241906.



- [18] K.J. Sankaran, N.H. Tai, I.N. Lin, *J. Appl. Phys.* 117 (2015) 075303.
- [19] J.T. Santos, T. Holz, A.J.S. Fernandes, F.M. Costa, V. Chu, J.P. Conde, *J. Micromech. Microeng.* 25 (2015) 025019.
- [20] D. Lu, H.D. Li, S.H. Cheng, J.J. Yuan, X.Y. Lv, *Nano Micro Lett.* 2 (2010) 56-59.
- [21] K.L. Ma, J.X. Tang, Y.S. Zou, Q. Ye, W.J. Zhang, S.T. Lee, *Appl. Phys. Lett.* 90 (2007) 092105.
- [22] K. Tahara, H. Ozawa, T. Iwasaki, N. Mizuochi, M. Hatano, *Appl. Phys. Lett.* 107 (2015) 193110.
- [23] T. Teraji, T. Ito, *J. Crys. Growth* 271 (2004) 409-419.
- [24] T.H. Chen, J. Wei, Y.H. Tzeng, *Diamond Relat. Mater.* 8 (1999) 1686-1696.
- [25] F. Silva, A. Gicquel, A. Tardieu, P. Cledat, Th. Chauveau, *Diamond Relat. Mater.* 5 (1996) 338-344.
- [26] H. Zhuang, L. Zhang, T. Staedler, X. Jiang, *Scripta Materialia* 65 (2011) 548-551..
- [27] H.A. Naseem, M.S. Haque, M.A. Khan, A.P. Malshe, W.D. Brown, *Thin Solid Films* 308-309 (1997) 141-146.
- [28] C.J. Tang, A.J.S. Fernandes, M. Granada, J.P. Leitão, S. Pereira, X.F. Jiang, J.L. Pinto, H. Ye, *Vacuum* 122 (2015) 342-346.
- [29] C.J. Tang, A.J. Neves, J. Grácio, A.J.S. Fernandes, M.C. Carmo, *J. Cryst. Growth* 310 (2008) 261-265.
- [30] Keith A. Snail, *Optical Mateirals* 1 (1992) 235-258.
- [31] X. Jiang, C.L. Jia, *Appl. Phys. Lett.* 80 (2002) 2269-2271.
- [32] K. Ichikawa, H. Kodama, K. Suzuki, A. Sawabe, *Thin Solid Films* 600 (2016) 142-145.
- [33] C.J. Tang, A.J. Neves, M.C. Carmo, *J. Phys.: Condens. Matter* 17 (2005) 1687-1695.
- [34] C.J. Tang, A.J. Neves, M.C. Carmo, *Appl. Phys. Lett.* 86 (2005) 223107.

- [35] C. Fang, X.P. Jia, N. Chen, Y.D. Li, L.S. Guo, L.C. Chen, H.A. Ma, X.B. Liu, *J. Cryst. Growth* 436 (2016) 34-39.
- [36] C.J. Tang, A.J.S. Fernandes, X.F. Jiang, J.L. Pinto, H. Ye, *J. Cryst. Growth* 434 (2016) 36-41.
- [37] C.J. Tang, I. Abe, L.G. Vieira, J. Gracio, J.L. Pinto, *Diamond Relat. Mater.* 19 (2010) 404-408.
- [38] J. Weng, L.W. Xiong, J.H. Wang, S.Y. Dai, W.D. Man, F. Liu, *Diamond Relat. Mater.* 30 (2012) 15.
- [39] C.J. Tang, J. Grácio, A.J. Neves, H. Calisto, A. J. S. Fernandes, Lianshe Fu, S. Pereira, L.P. Gu, Cabral Gil, M.C. Carmo, *J. Nanosci. Nanotech.* 10 (2010) 2722-2730.
- [40] G. Lombardi, K. Hassouni, G.D. Stancu, L. Mechold, J. Röpcke, A. Gicquel, *J. Appl. Phys.* 98 (2005) 053303.
- [41] Z. Yiming, F. Larsson, K. Larsson, *Theor. Chem. Acc.* 133 (2014) 1432 (12 pages).
- [42] B.S. Truscott, M.W. Kelly, K.J. Potter, M. Johnson, M.N.R. Ashfold, Y.A. Mankelevich, *J. Phys. Chem. A* 119 (2015) 12962-12976.

**Fig. 1** High-resolution SEM micrographs of the three NCD samples grown with N<sub>2</sub> additive on 1 mm thick Si slices at different microwave power: 3.0 kW (a, b), 3.5 kW (c, d) and 4.0 kW (e, f).

**Fig. 2** The absorbance FTIR spectra of the three NCD films grown with N<sub>2</sub> additive on 1 mm thick Si slices at different microwave power: 3.0 kW (ND1), 3.5 kW (ND2) and 4.0 kW (ND3).

**Fig. 3** Enlarged CH stretching band of the three NCD films grown with N<sub>2</sub> additive on 1 mm thick Si slices at different microwave power: 3.0 kW (ND1), 3.5 kW (ND2) and 4.0 kW (ND3).

**Fig. 4** (a) The absorbance FTIR spectrum of the ND4 film grown with N<sub>2</sub> additive on Si wafer of 5.08 in diameter and 3.26 mm thick at power 3.0 kW, and (b) the top part of the enlarged CH stretching band after removing the baseline marked in (a).

**Table 1** Some of the growth parameters and characteristics of the N-doped NCD films studied here: A<sub>CH</sub> stands for the integrated area of CH stretching band, average grain size was calculated based on the XRD measurements.

Sample	Power (kW)	Si thickness (mm)	N <sub>2</sub> (sccm)	Thick ness ( $\mu\text{m}$ )	Gr. Rate ( $\mu\text{m}/\text{h}$ )	Av. grain size (nm)	A <sub>CH</sub>	A <sub>CH</sub> /t	I <sub>2833</sub> / I <sub>2920</sub>
ND1	3.0	1.0	1.0	29	5.4	47	42.82	14765	1.03
ND2	3.5	1.0	1.6	40	7.1	38	68.30	17075	1.08
ND3	4.0	1.0	1.6	45	9.6	34	57.16	12702	1.02
ND4	3.0	3.26	1.0	87	3.5	31	100.12	11508	1.15

**Table 2** Sharp peaks observed in the CH stretching band of the NCD films grown with a small amount of pure N<sub>2</sub> additive into 4 % CH<sub>4</sub>/H<sub>2</sub> plasma and the corresponding assignment of the peaks.

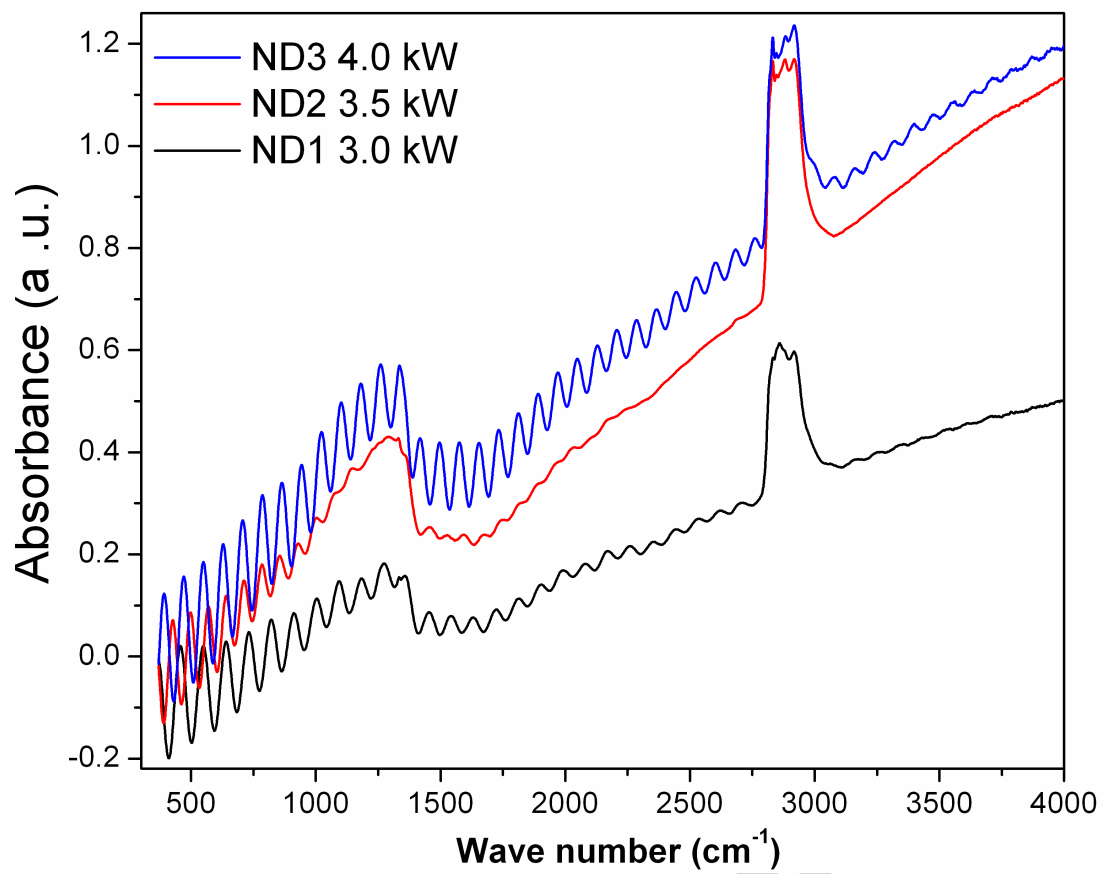
Samples	?	sp <sup>3</sup> CH <sub>2</sub>	sp <sup>3</sup> CH <sub>3</sub>	sp <sup>3</sup> CH	sp <sup>3</sup> CH <sub>2</sub>
ND1	2833		2860	2871	2918
ND2	2831	2846		2881	2918
ND3	2832	2848		2883	2916
ND4	2833	2849	2859	2877	2918

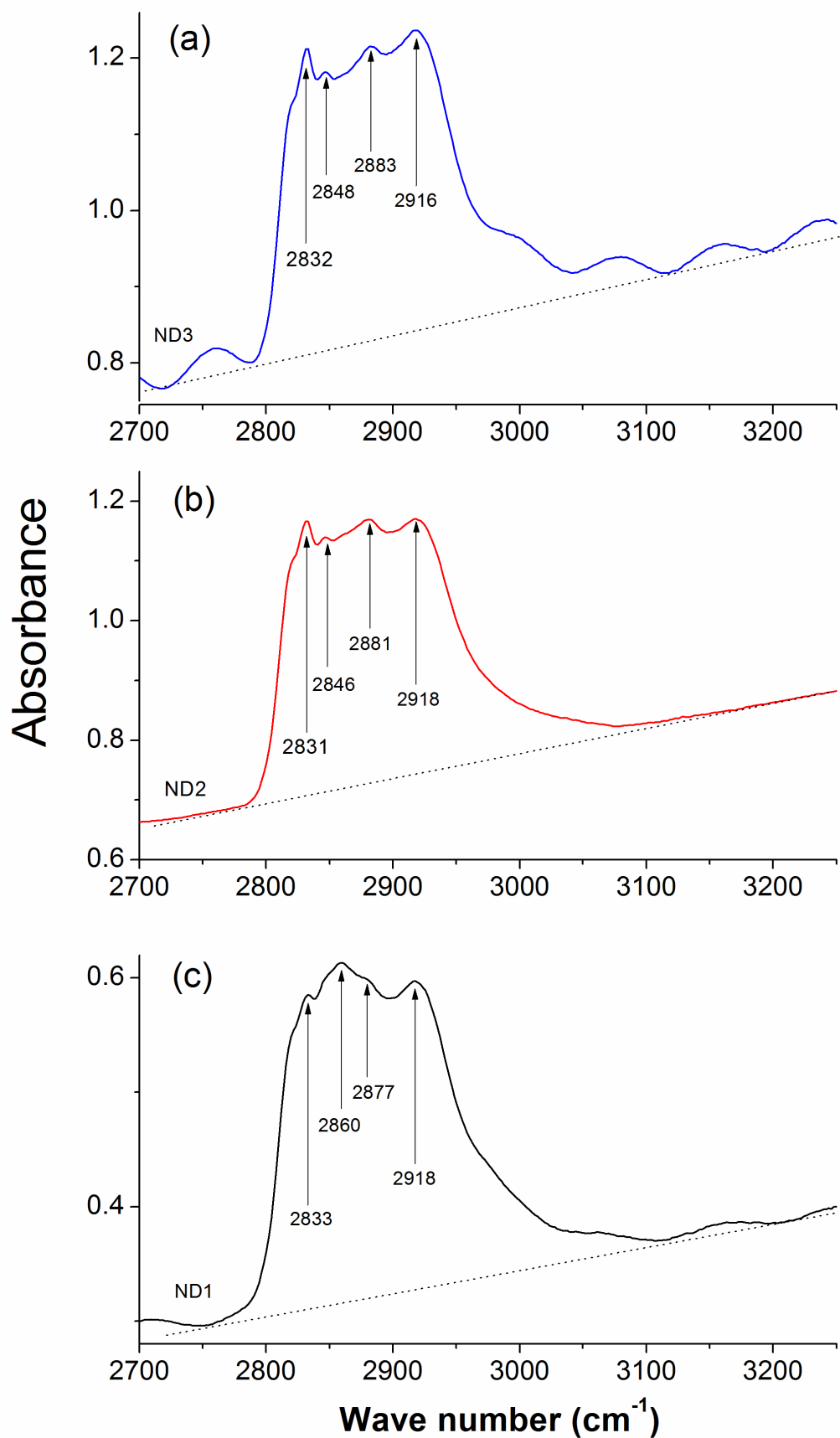
**Table 3** Comparison of the effect of various growth parameters such as microwave power (associated substrate temperature  $T_s$ ) and  $N_2$  on H incorporation in NCD films based on the present and our previous related work namely Ref. 36 and 37. ( $t_{Si}$  means the thickness of Si substrate)

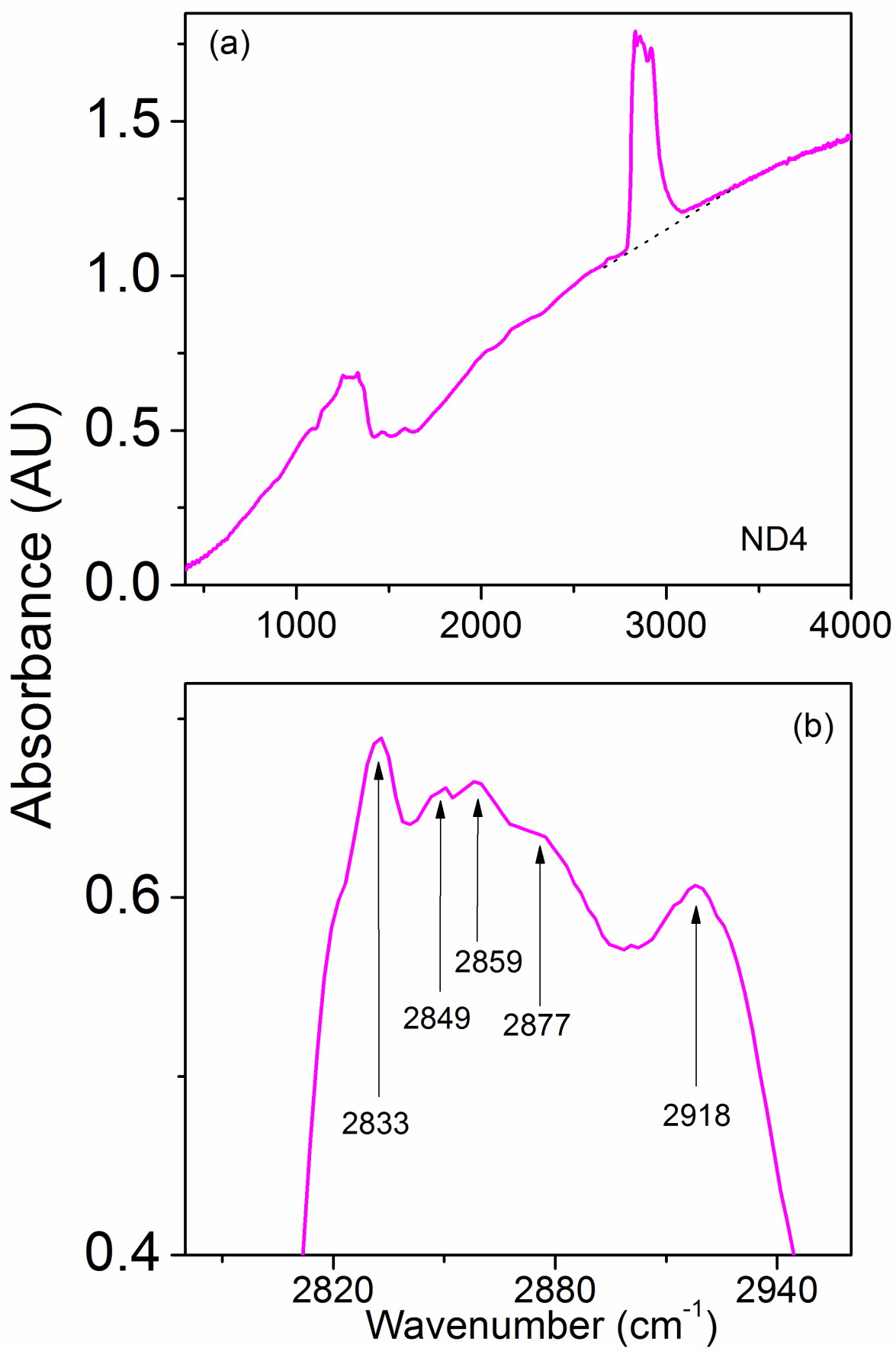
Variables	Power (kW) ( $\Delta T_s$ (°C))	$N_2$ (sccm)	Trend of H content	Source
MP ( $T_s$ ), $N_2$	3.0 ↗ 3.5 ( $T_s$ ↗ 41)	1.0 ↗ 1.6	↑	ND2 vs. ND1
MP ( $T_s$ ), $N_2$	3.0 ↗ 4.0 ( $T_s$ ↗ 64)	1.0 ↗ 1.6	↓	ND3 vs. ND1
MP ( $T_s$ )	3.5 ↗ 4.0 ( $T_s$ ↗ 23)	1.6	↓	ND3 vs. ND2
MP ( $T_s$ )	2.0 ↗ 3.2 ( $T_s$ ↗ 72)	<b>0.8</b> [ $O_2$ 0.2]	↓	Ref. 34
$N_2$ [ $O_2$ ]	3.0 ( $T_s$ )	0 ↗ <b>1.0</b> [ $O_2$ 1.0 ↘ 0]	↑	Ref. 35
$t_{Si}$ ( $T_s$ )	3.0 ( $T_s$ ↗ 116)	1.0	↓	ND4 vs. ND1

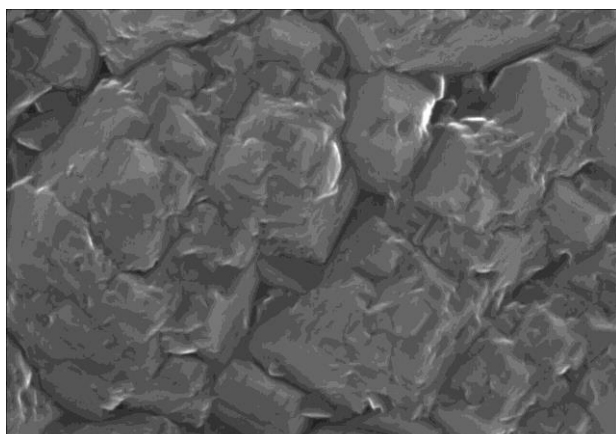
### Highlights

- First study of H defects in NCD films grown with  $N_2$  additive in  $CH_4/H_2$  plasma by FTIR
- The new H related sharp absorption peak appears stronger with increasing power  $>3$  kW
- NCD films grown with  $N_2/CH_4/H_2$  plasma at high powers have a large amount of H defects

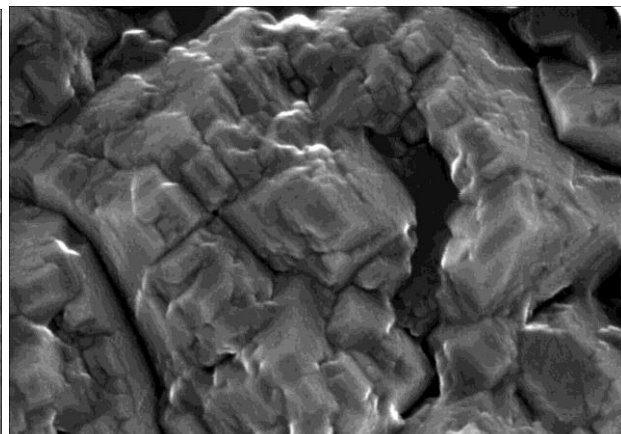




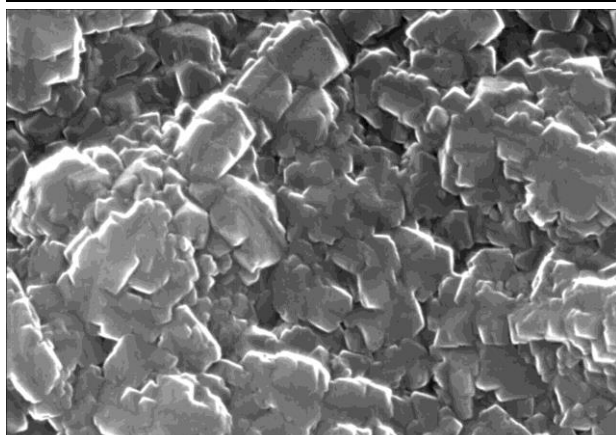




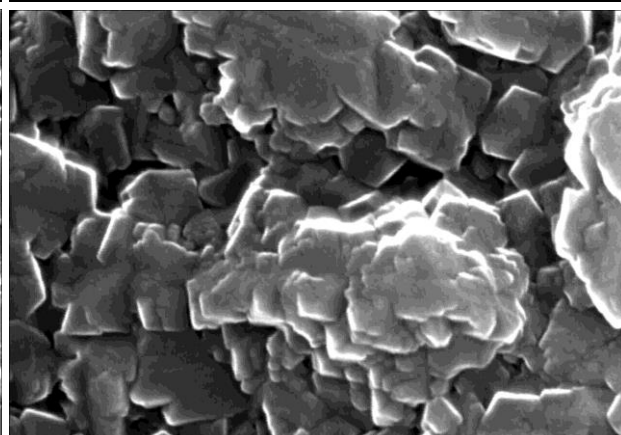
SU70 25.0kV 8.3mm x60.0k SE(M)



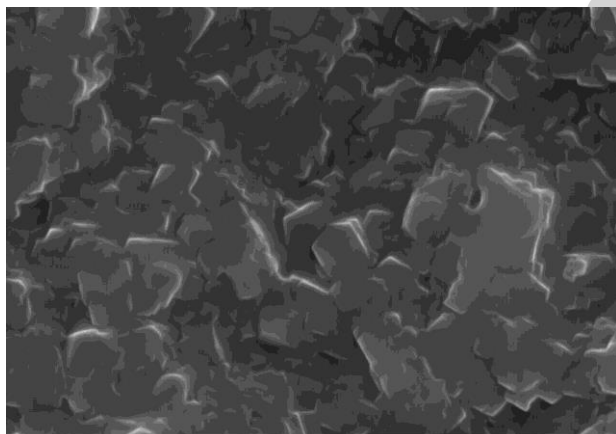
SU70 25.0kV 8.3mm x100k SE(M)



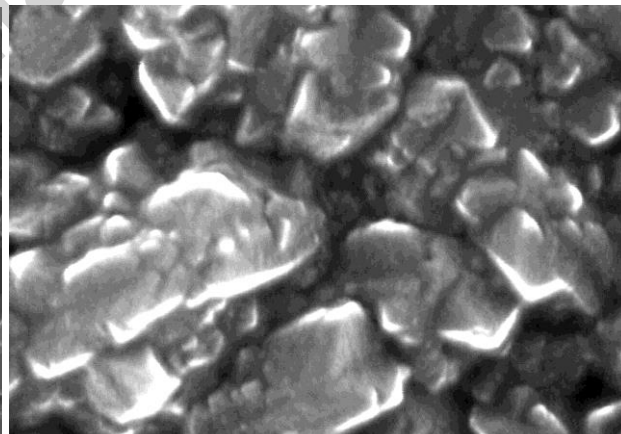
SU70 25.0kV 9.3mm x60.0k SE(M)



SU70 25.0kV 9.3mm x100k SE(M)



SU70-94 15.0kV 8.9mm x60.0k SE(M)



SU70-95 15.0kV 5.9mm x120k SE(M)